Journal of Rock Mechanics and Tunnelling Technology (JRMTT)
31(2) 2025 pp 107-119

Available online at www.isrmtt.com

Assessment of Single Shield TBM Performance Through the Phyllite Formations of Uttarakhand Himalayas - A Case Study

*Majid Tajik[1]**
Sumit Jain[2]
Mohammad Forooghi[1]

[1]Turkish Engineering Consulting & Contracting - TÜMAŞ India Pvt. Ltd.
Gurugram, India
[2]Rail Vikas Nigam Ltd., New Delhi, India

**Email: majid.tajik@tumas.com.tr*

ABSTRACT

This study focuses on the assessment of Single Shield Tunnel Boring Machine (TBM) performance in the context of phyllite rocks of the Himalaya region. The Q_{TBM} and NTNU models are well-known prediction models in the field of hard rock TBMs. In this study, the actual performance of two single TBMs with a diameter of 9.11m is compared with these models. The study of approximately 3km of tunnel excavation in the Rishikesh-Karnprayag Broad Gauge Rail Link project (Package 4) reveals that in phyllite rocks, owing to their heterogeneous structure, the correlation between the point load index and the field penetration index (FPI) is 0.19 and among the two models investigated, the NTNU model demonstrates greater consistency with the actual TBM performance.

Keywords: Single shield TBM; Phyllite; Q_{TBM}; NTNU; Penetration rate; Point load strength index.

1. INTRODUCTION

Tunnel Boring Machines (TBMs) are commonly used in long tunnel projects such as highway, hydropower, railway, and metro tunnels, where project schedules and precise boring operations are paramount. The evaluation of TBM performance is critical to increasing tunnel progress and ensuring cost-effectiveness. In fact, mechanized tunneling is the reaction between the machine and ground. Hence, the two groups of data are affecting TBM performance. The first category is related to machine specification and operating parameters and the second pertains to the ground conditions encountered during boring.

In the context of Himalayan geological conditions, certain experiences pertaining to TBM tunneling have been documented, wherein the use of TBM was not encouraging (Goel, 2014). This research is based on experimental methods NTNU (Trondheim Norwegian University of Science and Technology) and Q_{TBM}, which enables the assessment of TBM performance by analyzing operational parameters and rock mass properties measured during the tunnel excavation. This approach allows project stakeholders to make informed decisions to enhance TBM performance and improve overall project outcomes.

2. BRIEF DESCRIPTION OF THE PROJECT

Rishikesh-Karnprayag Railway Project is a 125km Broad Gauge new rail line between Rishikesh and Karnprayag in the state of Uttarakhand, India, which will facilitate freight and passenger traffic in this region. Rail Vikas Nigam Limited (RVNL) is a Public Sector Enterprise created by the Ministry of Railways, Government of India, and takes the responsibility of implementing this Project.

Tunnel 8 (Twin tunnel of lengths 14.61km each) of Rishikesh-Karnprayag railway is planned to be constructed by part New Austrian Tunneling Method (NATM) on both sides of the portals and part by TBM in the middle portion of the tunnels (Bansal et al., 2023). Two single shield TBMs with 9.11m diameter (Fig. 1) are applied for the excavation of main tunnel upline of 10,560 m and main tunnel downline of 10,475m. The selection of these machines has been guided by the geological characteristics and rock mass properties along the tunnel alignment. Geotechnical investigations indicate that phyllite formations exhibit a potential for squeezing. To mitigate the risk of the TBM getting stuck, the client has proposed the use of a single shield TBM.

Figure 1 - Assembly of the single shield TBM at the Devprayag portal of the tunnel

The final lining of the tunnels consists of (1+7) universal precast concrete segments with a thickness of 450mm and an average width of 1700 mm, which are installed by the machine continuously. Already, 1865m of upline tunnel and 980m of downline tunnel have been constructed and this paper evaluates the performance of TBMs in this section. Some TBM specifications are given in
Table 1.

Table 1 - Specifications of TBMs for upline and downline tunnel excavation

Manufacture	Herrenknecht, Germany
Model	Single shield TBM S1309A, S1310A
Cutter head diameter	9.11m
Disc cutter size / Number	19inch / 55
Cutter rotation speed	0-11 rpm
Shield length	10.67m
Nominal thrust	108,619 kN @ 420 bar
Number of thrust cylinders	42
Ring building	Universal Segment (7 + Key)
Ring length	1700mm

3. GEOLOGICAL FEATURES

The project area is located in Garhwal region. The Garhwal region of western Himalaya, lying between the Kali River in the east and the Yamuna River in the west, includes a 320 km stretch of mountainous terrain.

As per the Himalayan Subdivision, the project is located in the Lesser Himalaya and includes a thrust-bound sector delineated by two tectonic plates: The Main Boundary Thrust (MBT) to the south and the Main Central Thrust (MCT) to the north (Valdiya, 1980). The general geological map of the study area is represented in Figure 2 (Valdiya, 1980). A number of folds like the Garhwal Syncline and Mussoorie syncline are developed in the Lesser Himalaya. The rocks of Chandpur and Garhwal Group have undergone three phases of folding producing prominent foliation planes and kink bands are extensively developed on the foliation planes. The phyllite of Chandpur Group of Central Crystalline appears to be poly-phased deformed and metamorphosed (Tumas India and Altinok JV, 2019).

The tunnel path predominantly includes the Chandpur Formation of the Jaunsar group. The main geological unit that is observed along the tunnel is the Chandpur Phyllite (Quartzitic Phyllite and Schistose Phyllite) rock formation. The phyllite unit includes quartz veins and the intercalation of quartzite rocks. The rock mass is grey to brown and grey to greenish in colour, closely to very closely jointed, foliated, slightly to moderately weathered, and moderately weak to moderately strong.

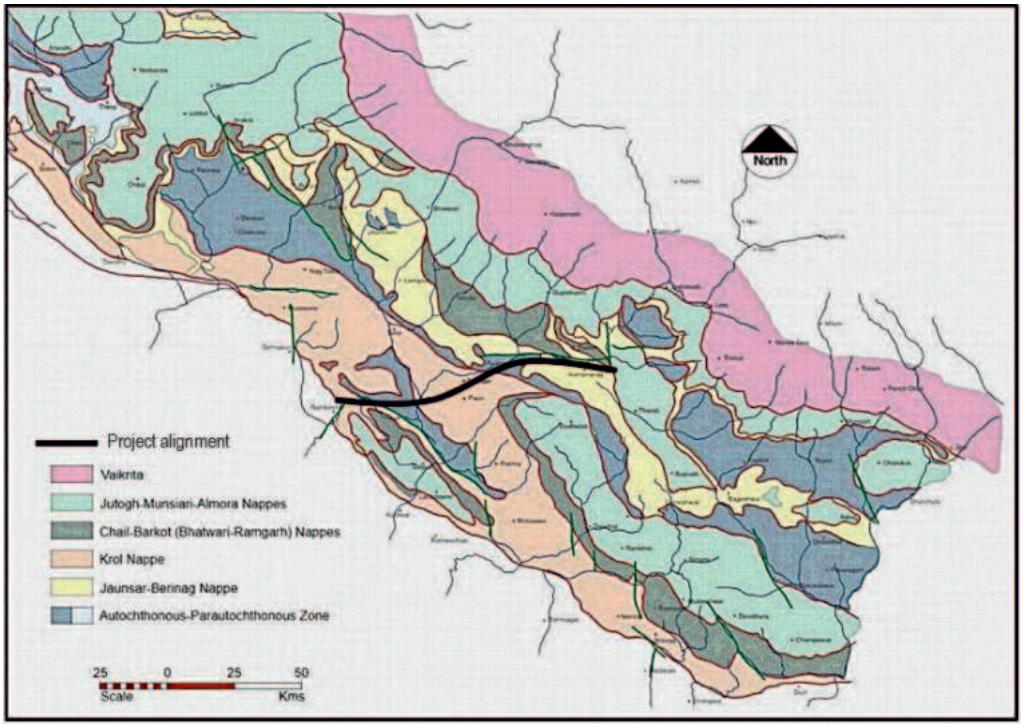

Figure 2 - Geological map of Lesser Himalaya (Valdiya, 1980)

4. DATA ASSESSMENT

In addition to existing geological documents such as geotechnical baseline report (GBR) and geotechnical data report; additional data related to ground condition and rock properties was collected and used through face mapping, muck assessment, core drilling, and laboratory tests (Fig. 3). Geological mapping and assessment of the tunnel face represent significant challenges in tunneling operations using hard rock TBMs. During active excavation, direct observation of the tunnel face is hindered by the continuous operation of the TBM. However, during downtime periods, such as maintenance shifts, it is possible to access the face. In such instances, the presence of the TBM itself obstructs the geologist's ability to observe the entire tunnel face and limits access to its complete surface (Fig. 4).

In recent years, advancements in technology have facilitated the use of modern digital cameras and photo/video analysis software, enabling a comprehensive evaluation of the tunnel face surface (Chen et al., 2021; Chuyen & Hyu-Soung, 2022; Gaich & Pötsch, 2016; Lemy & Hadjigeorgiou, 2004). Considering that the efficiency of single TBMs are usually not more than 30% (Rostami, 2016), there is enough opportunity to face mapping.

Figure 3 - Geological and geotechnical investigations during TBM operation, (a) point load test (b) muck assessment during mining (c) rock core drilling and logging (d) face mapping

Table 2 summarizes the geological data and geotechnical properties obtained through muck assessment and laboratory testing. RQD was observed to be in the range of 0-55%.

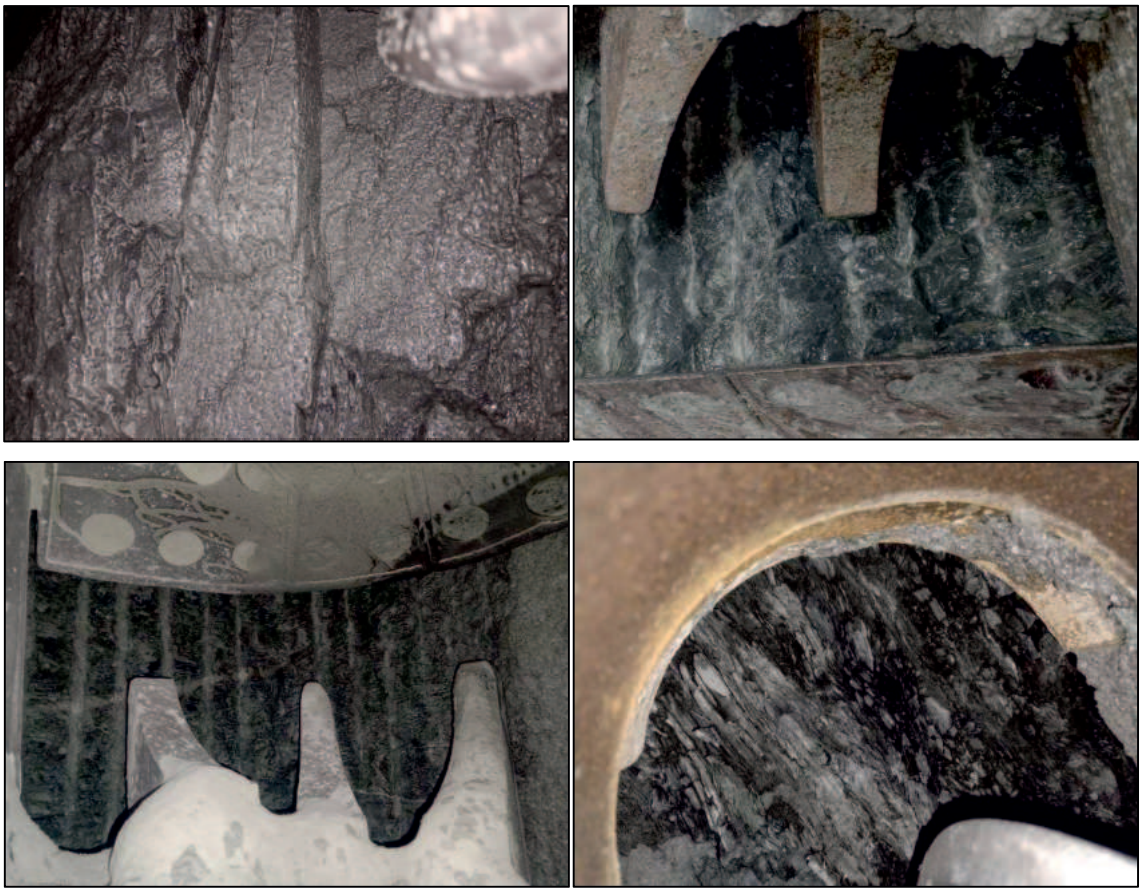

Figure 4 – Different views of face mapping in hard rock single shield TBM

Table 2 - Ground investigation techniques used to assess geological and geotechnical conditions

Geological data and geotechnical properties	Ground investigation	
	Muck assessment	Laboratory test
Lithology	Quartzitic Phyllite, Schistose Phyllite, and Quartzite	
Ground Water condition	Dry to Flowing	—
Geological hazard (cavity, fault, fractured zone)	This relies on probe drilling, the interpretation of MWD data, and observations from geologists.	—
Weathering	Fresh to highly weathered	—
Joint condition (J_r, J_n, J_w, J_a)	J_r = 2-3; J_n = 4-12; J_w = 0.5 - 1; J_a = 1-8	—
Point load index (MPa)		1.41-3.61
Density (g/cm^3)		2.33-2.47
Cerchar abrasiveness index (CAI)		1.41 - 4.24

In this project, both single shield TBMs are equipped with a real-time data recorder, which was recording all boring parameters. Activities and delays are also recorded on a shift basis. The daily advance rate and cumulative progress of both upline and downline TBMs are recorded and are shown in Figures 5 & 6 respectively for comparison.

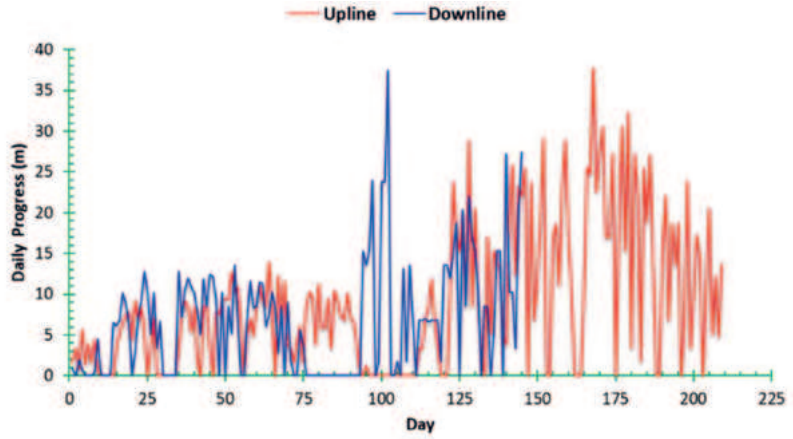

Figure 5 - Comparing the daily progress of upline (UL) and downline (DL) TBMs

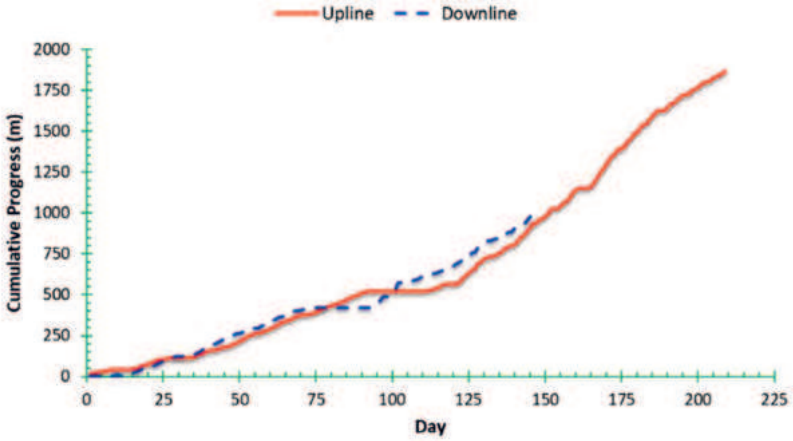

Figure 6 - Comparing the cumulative advance/progress of upline and downline TBMs

In general, in most TBM tunneling projects, the progress rate is low in the initial excavation stages due to logistical constraints, limited workforce expertise, and incomplete knowledge of the geological characteristics along the tunnel route.

The most significant factors contributing to an increase in the utilization factor and, consequently, the progress rate after the training period are:

- As excavation advances and the TBM backup system moves farther from the portal, transportation system constraints and loading/unloading limitations are mitigated.
- Operator proficiency in segmental ring erection improves, reducing downtime in concrete lining installation.
- The ratio of unscheduled breakdowns to TBM boring time decreases after the training period. This ratio is initially 1.0 during the training phase but declines to 0.324 as excavation progresses (USACE, 1997), indicating improved personnel competency in managing unscheduled breakdowns.

As illustrated in Figure 6, the increase in the advance rate after the training period (the first 100 days of TBM operation) is primarily attributed to a higher utilization factor, which results from greater experience and more efficient management of TBM activities. The key factors contributing to the increase in the utilization factor and consequently, the advance rate in the upline (UL) and downline (DL) tunnels include:

- Installation of a permanent conveyor belt and an optimized mucking system in both the tunnel portal and the TBM backup system. The permanent conveyor belt replaced the temporary unloading system in upline and downline TBMs on operational days 93-111 and 76-93, respectively (Fig. 6).
- As illustrated in Fig. 7, the installation time per segmental ring for both TBMs decreases as machine operating days increase and tunnel advancement progresses. To enhance the clarity of the charts, TBM operation days without segmental ring installation have been excluded from the analysis.

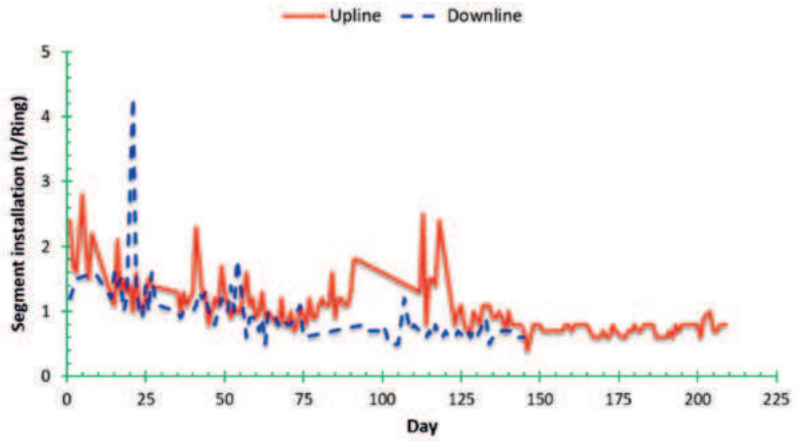

Figure 7 - Relationship between segmental ring installation time and operational days for both TBMs

Figure 8 illustrates the distribution of downtimes for both TBMs. The average utilization factor for the 2,845m tunnel excavation is 18.98%, with the majority of downtimes attributed to support installation, shift changes, and transportation. Notably, delays in support installation are expected in the case of a single TBM operation.

Rate of penetration (ROP) is also referred to as penetration rate (PR) and often expressed in m/h and refers to the linear footage of excavation per unit time, when machine engages the ground and is in production (Rostami, 2016). In other words, the rate of penetration can be defined as the ratio of the length of tunnel excavation (L) to the duration of a single boring stage (t_B). This metric quantifies the cutterhead advance in the rock mass until the commencement of the next operational phase and is expressed in m/h, as per Equation 1. Figure 9 illustrates a comparative graph of the penetration rate measurements obtained from both TBMs.

$$ROP = \frac{L}{t_B} \quad (1)$$

where

L = Length of tunnel excavation in m, and

t_B = time of excavation in a single boring phase in hours.

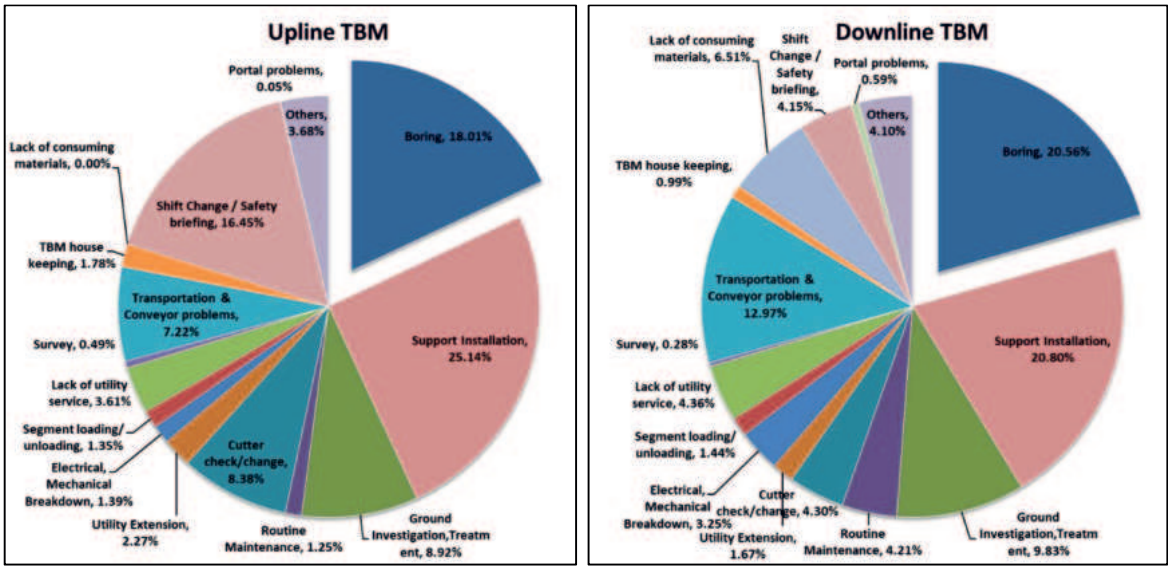

Figure 8 - Distribution of downtimes of both TBMs in upline and downline tunnel excavation

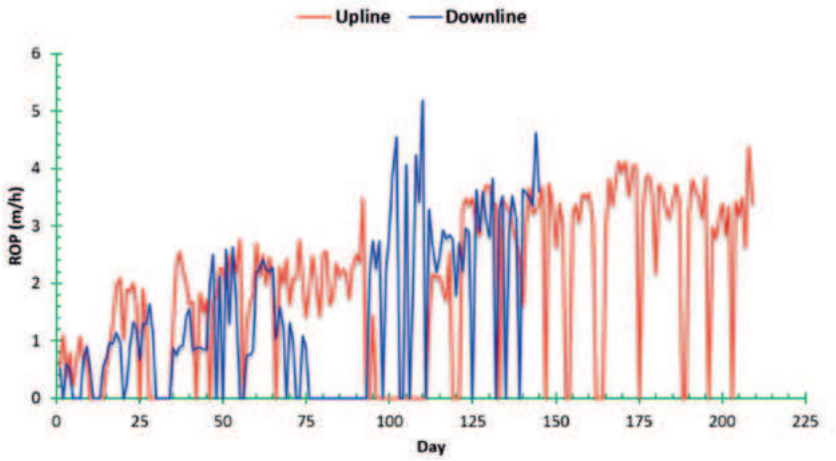

Figure 9 - Comparative penetration rate of upline and downline TBMs

The penetration rate can be alternatively assessed concerning the indentation depth of the disc cutter for each revolution of the cutterhead, denoted as mm/rev. In this case, with considering the rotational speed of the cutterhead (RPM), it can be equivalently expressed in units of mm/min. This parameter is notably influenced by the thrust force exerted upon the disc cutters, as well as the compressive strength of the intact rock. Its value increases with the augmentation of the thrust force of TBM, as illustrated in Figure 10. In order to ascertain the compressive strength of the intact rock, the point load test was employed according to the ASTM- D 5731-02 standard. Specimens in the form of rock cores, blocks, or irregular lumps can be tested by this test method (ASTM, 2008). In mechanized tunneling, the point load index mainly resulted from irregular specimens that were collected during mucking.

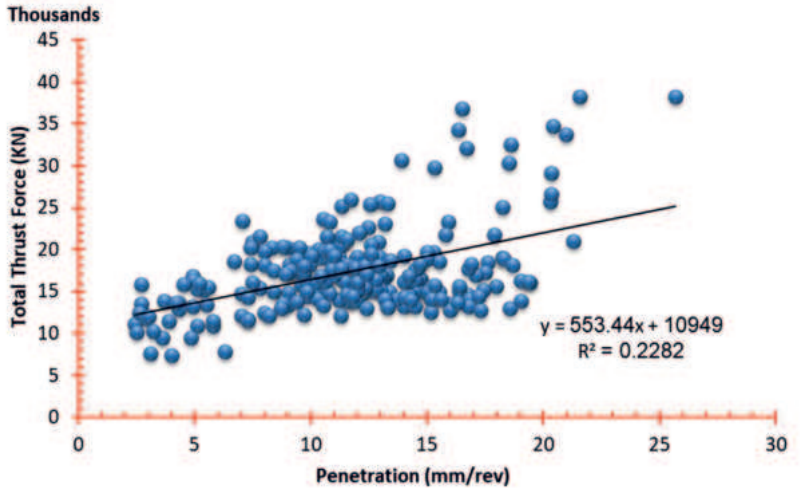

Figure 10 - Comparative penetration rate of upline and downline TBMs

In the evaluation of TBM performance, numerous parameters come into play, often necessitating the utilization of composite parameters for a comprehensive understanding of their interdependencies. This research focuses on employing the field penetration index (FPI) as a pertinent composite parameter to assess the influence of point load strength in Himalayan phyllites on TBM performance.

The FPI is influenced by the thrust force applied by the TBM to each disc cutter as well as the penetration rate, as defined by Equation 2 (Barton, 2000).

$$FPI = \frac{thrust\ /cutter\ \ (kN)}{penetration\ \ \ rate\ \ (mm\ /rev)} \tag{2}$$

In this equation, the thrust/cutter is calculated by dividing the total normal force by the number of disc cutters engaged on the cutterhead, while the penetration rate represents the depth of cutterhead advance into the rock per revolution.

As shown in Figure 11, FPI increases with an increase in the Point Load Strength Index, but the coefficient of determination (R^2) for this relationship is 0.19. The main reason for this correlation is the heterogeneity of the phyllite rock. This can be explained by the fact that the Himalayan Phyllites in this section of the tunnel exhibit a foliated and highly folded structure, with this foliation serving as a weakness plane. Consequently, $I_{S(50)}$ varies when specimens are loaded either parallel, perpendicular, or at unknown/random directions in relation to these weakness planes.

5. TBM PERFORMANCE EVALUATION

In this study, TBM performance has been evaluated through the implementation of an experimental method inspired by NTNU and Q_{TBM} approaches considering the properties of phyllite. The NTNU model has been developed by the Norwegian University of Science and Technology since 1976 and the current model is based on data from 35 projects with more than 250km of tunnels (Bruland, 2000).

The parameters used in this method include the TBM parameters (such as thrust force, rotation speed, cutter spacing, and cutter size) and rock mass properties (fracturing, drilling rate index, porosity). The penetration rate is estimated as per Equations 3 and 4.

$$i_0 = (M_{ekv}/M_1)^b \text{ (mm / rev)} \quad (3)$$

$$I_0 = i_0 RPM(60/1000) \quad \text{(m / h)} \quad (4)$$

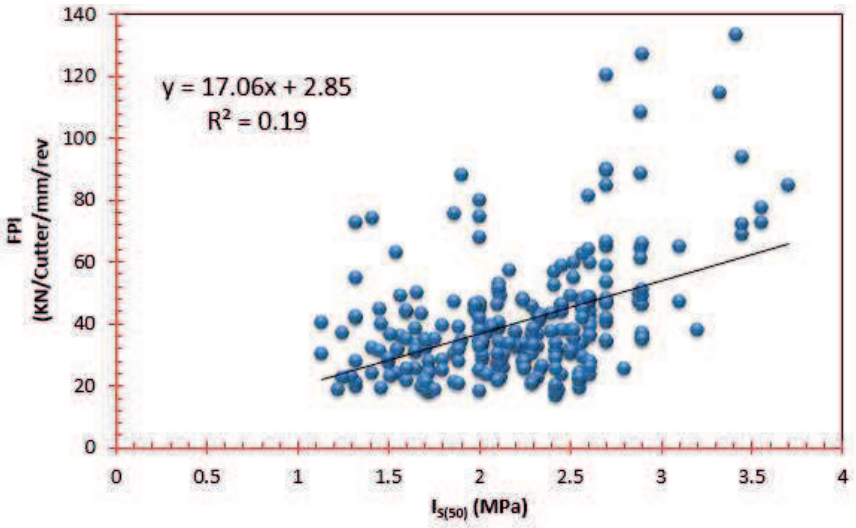

Figure 11 - Relationship between point load strength index and field penetration index (FPI) on Himalayan phyllites

In above equations i_0 is basic penetration rate; M_{ekv} is the equivalent cutter thrust factor, which is obtained by dividing the total thrust force by 55 cutters, M_1 is critical cutter thrust (necessary thrust to achieve 1mm/rev), b is penetration coefficient, I_0 is a function of basic penetration and cutterhead rpm. Critical cutter thrust (M_1) and penetration coefficient (b) are calculated based on equivalent fracturing factor (EFF), which depends on the combination of parameters such as systematic discontinuities, degree of jointing, the angle between discontinuity planes and the tunnel direction, porosity, and the drillability index of the intact rock.

Q_{TBM} model was established on Q-system and suggested to estimate TBM penetration as per Equations 5 and 6. This model is strongly based on the familiar Q parameters but has additional rock-machine-rock mass interaction parameters. The conventional Q-value, together with the cutter life index and quartz content help to explain some of the delays involved (Barton, 1999).

$$Q_{TBM} = \left(\frac{RQD_0}{J_n}\right) \times \left(\frac{J_r}{j_a}\right) \times \left(\frac{J_w}{SRF}\right) \times \left(\frac{SIGMA}{F^{10}/_{20^9}}\right) \times \left(\frac{20}{CLI}\right) \times \left(\frac{q}{20}\right) \times \left(\frac{\sigma_\theta}{5}\right) \quad (5)$$

$$PR = 5 \times Q_{TBM}{}^{(-0.2)} \quad \text{(m/h)} \quad (6)$$

where

RQD_0 = rock quality designation in the direction of the tunnel excavation,

J_n = joint set number,

J_r = joint roughness number for critically oriented joint set,
J_a = joint alteration number for critically oriented joint set,
J_w = joint water reduction factor,
SRF = stress reduction factor to consider in situ stresses and according to the observed tunneling conditions (Singh & Goel, 2011),
SIGMA = rock mass strength estimate (MPa),
F = average cutter load (tnf) through the same zone, normalized by 20 tnf,
CLI = cutter life index,
q = quartz content percentage,
σ_θ = induced biaxial stress on tunnel face (MPa) in the same zone, normalized to an approximate depth of 100m, and
PR = penetration rate.

The actual rate of penetration was determined by dividing the daily advance by the recorded boring time for both TBMs on a regular basis. During the comparison of the actual penetration rates with the NTNU and Q_{TBM} models, zero values associated with TBM parameters and rock properties were excluded. Furthermore, necessary conversions and adjustments were made using theoretical and experimental formulas.

The relationship between the actual ROP and the calculated ROP is shown in Figures 12 & 13 for the NTNU and Q_{TBM} models, respectively. In both models, the average ROP for tunnel excavation exceeds the actual ROP. This difference is more pronounced in the Q_{TBM} model than in the NTNU model. In other words, the NTNU model exhibits better compliance with the TBM penetration rate in Himalayan phyllites. One of the factors contributing to variations in the actual penetration rate of the TBM is associated with the thrust force exerted on the cutters. A portion of this force is allocated to overcome the friction between the TBM shield and the ground, and the amount of shield friction depends on the geological conditions and the design details of the TBM.

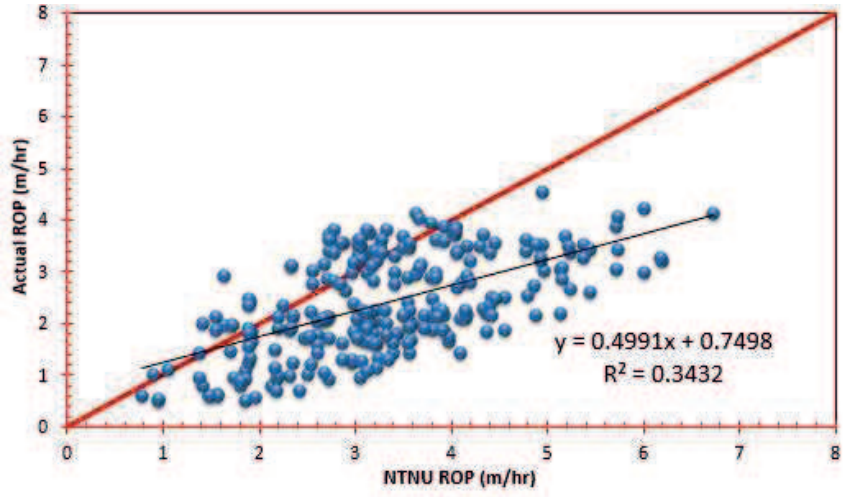

Figure 12 - Relationship between actual and NTNU penetration rate

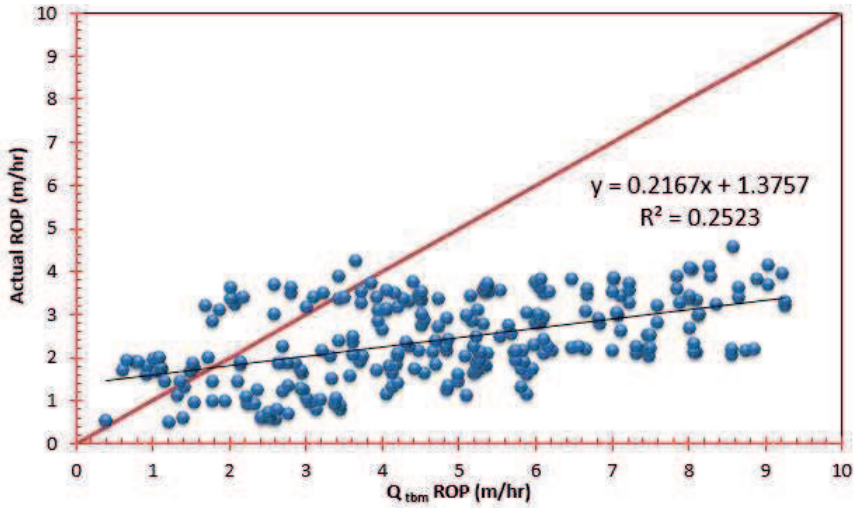

Figure 13 - Relationship between actual and Q_{TBM} penetration rate

6. CONCLUSIONS

- Based on data obtained from approximately 3km of tunnel in Himalayan phyllites, a comparison was made between the results of two most commonly used TBM performance prediction models (NTNU and Q_{TBM}) and actual performance of TBM. The results indicate that the Q_{TBM} model does not adequately represent actual TBM performance under these geological conditions and is therefore not suitable for phyllitic formations. In contrast, the NTNU model demonstrates a stronger correlation with observed TBM performance. With appropriate adjustments, it can provide more accurate predictions for the remaining tunnel sections. The improved conformity of the ROP_{Actual} with the ROP_{NTNU} in the NTNU model can be attributed to the model's consideration of foliation characteristics, including strike and spacing. These geological parameters are incorporated into the NTNU model through the equivalent fracturing factor, enhancing its predictive capability in phyllitic formations.
- While in this part of the tunnel, point load strength and ROP exhibit a direct relationship, it appears that the heterogeneity of the phyllites, coupled with their folded structural characteristics, significantly influenced the ROP, subsequently affecting the coefficient of determination. To validate this effect, it is crucial to perform more precise face mapping and rock mass classification during TBM downtimes by utilizing advanced technologies, such as video cameras and image processing software. This approach will enable a more thorough assessment of the impact of foliation direction on both the rate of penetration and point load strength.

DISCLOSURES

The authors declare that they have no conflicts of interest related to this work.

ACKNOWLEDGMENTS

The authors would like to express their gratitude to Larsen & Toubro Company, with special appreciation for the invaluable assistance provided by the Geology Department in facilitating the collection of essential data.

References

ASTM, D-5731 (2008). Standard Test Method for Determination of the Point Load Strength Index of Rock and Application to Rock Strength Classifications. American Society for Testing and Materials, West Conshohocken, PA, USA.

Bansal V, Patle S, Bhardwaj HA (2023). Design and construction sequence of big crossover cavern in Himalayan Geology. Proc of the ITA-AITES World Tunnel Congress (WTC), CRC Press, 978-1-003-34803-0, 452-459.

Barton NR (1999). TBM performance estimation in rock using Q_{TBM}. Tunnel & Tunnelling International, 31(90): 30-34.

Barton NR (2000). TBM Tunnelling in Jointed and Faulted Rock. CRC Press, IS BN 905809 34 17, AA Balkema, Rotterdam, 23p.

Bruland A (2000). Hard Rock Tunnel Boring - Advance Rate and Cutter Wear. PhD Thesis at NTNU, Norway, Vol. 3.

Chen J, Yang T, Zhang D, Huang H, Tian Y (2021). Deep learning-based classification of rock structure of tunnel face. Geoscience Frontiers, 12(1):395-404.

Chuyen P, Hyu-Soung S (2022). 3D tunnel face modelling for discontinuities characterization: A comparison of Lidar and Photogrammetry Methods. Tunnel and Underground Space, 32(6): 549-557.

Gaich A, Pötsch M (2016). 3D images for digital tunnel face documentation at TBM headings–Application at Koralm tunnel lot KAT2/3D. Geomechanics and Tunnelling, 9(3), 210-221.

Goel RK (2014). Tunnel boring machines in the Himalayan tunnels. 5th Indian Rock Conference Indorock 2014, 1522-1532.

Lemy F, Hadjigeorgiou J (2004). A digital face mapping case study in an underground hard rock mine. Canadian Geotechnical Journal, 41(6):1011-1025.

Rostami J (2016). Performance prediction of hard rock tunnel boring machines (TBMs) in difficult ground. Tunnelling and Underground Space Technology, 57:173-182.

Singh B, Goel RK (2011). Engineering Rock Mass Classification; Tunnelling, Foundations, and Landslides, Butterworth-Heinemann Elsevier, UK, 365p.

Tumas India, Altinok JV (2019). Geotechnical baseline report (GBR). Part B, Package 4, RVNL, 8p.

USACE (1997). Tunnels and shafts in rock. Washington, DC, US Army Corps of Engineers, Engineering and Design.

Valdiya KS (1980). Geology of the Kumaun Lesser Himalaya. Wadia Institute of Himalayan Geology, Dehradun, 291p.